**Biogeosciences
Discussions**

Impacts of dust deposition on dissolved trace metal concentrations (Mn, Al and Fe) during a mesocosm experiment

K. Wuttig[1], T. Wagener[1,*], M. Bressac[2,3], A. Dammshäuser[1], P. Streu[1], C. Guieu[2,3], and P. L. Croot[1,**]

[1]Helmholtz Centre for Ocean Research Kiel (GEOMAR), FB2 Marine Biogeochemistry, Chemical Oceanography, Kiel, Germany
[2]Laboratoire d'Océanographie de Villefranche/Mer, CNRS-INSU, UMR7093, Observatoire Océanologique, 06230, Villefranche-sur-Mer, France
[3]Université Pierre et Marie Curie-Paris 6, UMR 7093, LOV, Observatoire Océanologique, France
[*]now at: Université d'Aix-Marseille, CNRS/INSU, IRD, Institut Méditerranéen d'Océanologie (MIO), UM 110, 13288 Marseille, France
[**]now at: Earth and Ocean Sciences, School of Natural Sciences, National University of Ireland, Galway (NUIG), Galway, Ireland

Correspondence to: K. Wuttig (kwuttig@geomar.de)

Impacts of dust deposition on dissolved trace metal concentrations

K. Wuttig et al.

Title Page

Abstract	Introduction
Conclusions	References
Tables	Figures

| ◄◄ | ►► |
| ◄ | ► |

Back | Close

Full Screen / Esc

Printer-friendly Version

Interactive Discussion

Abstract

The deposition of atmospheric dust is the primary process supplying trace elements abundant in crustal rocks (e.g. Al, Mn and Fe) to the surface ocean. Upon deposition, the residence time in surface waters for each of these elements differs according to

5 their chemical speciation and biological utilization. Presently however their behavior after atmospheric deposition is poorly constrained, principally because of the difficulty in following natural dust events in-situ. In the present work we examined the temporal changes in the biogeochemistry of crustal metals (in particular Al, Mn and Fe) after an artificial dust deposition event. The experiment was contained inside trace metal clean

10 mesocosms (0–12.5 m depths) deployed in the surface waters of the Northwestern Mediterranean, close to the coast of Corsica in the frame of the DUNE project (a DUst experiment in a low Nutrient low chlorophyll Ecosystem). Two consecutive artificial dust deposition events, each mimicking a wet deposition of $10 \, \mathrm{g \, m^{-2}}$ of dust, were performed during the course of this DUNE-2 experiment. The changes in dissolved manganese

15 (dMn), iron (dFe) and aluminium (dAl) concentrations were followed immediately and over the following week and their inventories and loss or dissolution rates were determined. The evolution of the inventories after the two consecutive additions of dust showed distinct behaviors for dMn, dAl and dFe. Even though the mixing conditions differed from one seeding to the other, dMn and dAl showed clear increases directly

20 after both seedings due to dissolution processes. Three days after the dust additions, dAl concentrations decreased as a consequence of scavenging on sinking particles. dAl appeared to be highly affected by the concentrations of biogenic particles, with an order of magnitude difference in its loss rates related to the increase of biomass after the addition of dust. For dFe concentrations, the first dust addition decreased the

25 concentrations through scavenging of the dust particles, whereas the second seeding induced dissolution of Fe from the dust particles. This difference, which might be related to a change in Fe-binding ligand concentration in the mesocosms, highlights the complex processes that control the solubility of Fe. Based on the inventories at the

mesocosm scale, the estimations of solubility of metals from dust particles in seawater were 1 % for Al and 40 % for Mn which were in good agreement with laboratory based estimates. Overall, the trace metal dataset presented here makes a significant contribution to enhancing our knowledge on the processes influencing trace metals release from Saharan dust and the subsequent processes of bio-uptake and scavenging in a low nutrient low chlorophyll area.

1 Introduction

Marine oligotrophic areas, also described as low nutrient, low chlorophyll (LNLC) areas, represent 60 % of the global ocean (Longhurst et al., 1995) and are suggested to contribute to 50 % of the oceanic carbon export (Emerson et al., 1997). These areas are characterized by low nutrient concentrations in oceanic surface waters resulting in reduced biological activity (Carr et al., 2006; Longhurst et al., 1995). Vast surfaces of these LNLC areas are subject to fluxes of lithogenic material through the atmospheric deposition of desert dust particles. Bioassay experiments performed in the oligotrophic North Atlantic by Mills et al. (2004) found that the addition of mineral dust to seawater can lead to a positive response in biota. Due to the elemental composition of the earth crust, the flux of dust particles constitutes a major source of trace metals to the surface ocean (Duce et al., 1991). For this reason, in addition to macronutrients (phosphorus and nitrogen) transported by dust particles, it has been suggested that the response of the biota to dust might be (partially) controlled by trace metals. During the last twenty years, due to its importance in HNLC areas, Fe has received much attention (Jickells et al., 2005), but in the recent years, a number of studies have pointed to the importance of studying other trace-elements in order to more completely describe the overall biogeochemical functioning of these LNLC area (Heller and Croot, 2010; Noble et al., 2008; Obata et al., 2008; Saito and Moffett, 2002).

In order to assess the impact of the atmospheric deposited micronutrients on the biogeochemical functioning of the LNLC areas, a variety of complex factors controlling

13859

the solubility of trace metals – from the solid form in a dust particle to the dissolved form once it enters the water – have to be taken into account (Baker and Croot, 2010). Indeed, in addition to atmospheric factors controlling the inherent solubility of the metal in the particle (size of the particles, Baker and Jickells, 2006; mineralogy, Journet et al.,

5 2008; chemical composition, Sedwick et al., 2007), there are a number of factors that can be important once the particle is deposited in seawater: e.g. the initial concentration of dissolved metals in seawater (Liu and Millero, 2002; Mendez et al., 2010), photochemical processing (Fe(III) to Fe(II)) (Zhuang et al., 1992) and availability in the atmosphere and in seawater (Spokes and Jickells, 1996), but also specific chelating

10 substances like for Fe (Gledhill and Buck, 2012; Wagener et al., 2008).

The Mediterranean Sea is a LNLC-area, especially in summer when the surface is strongly stratified. The atmospheric load over the Mediterranean has been estimated to reach up to one billion tonnes per year, which is one of the highest dust loads reaching a LNLC-area. For this reason the Mediterranean is a suitable place to assess the

15 impact of dust deposition on LNLC areas (Guerzoni et al., 1999). This is the objective of the project DUNE (a DUst experiment in a low Nutrient low chlorophyll Ecosystem) based on an original experimental approach: dust addition experiments into large clean mesocosms. This experimental design constitutes an opportunity to study processes once particles have deposited at the surface ocean in a realistic way (Guieu et al.,

20 2009, 2010a).

Within a first experimental campaign in 2008 (DUNE-1), it was demonstrated that the mesoscosms developed in the frame of the DUNE project allowed trace metal clean conditions adapted to study the Fe cycle (Wagener et al., 2010) Two major results concerning Fe chemistry were gained from this first experiment:

25 1. A clear decrease of the dissolved iron (dFe) inventory in the mesocoms, in which a wet deposition was simulated, compared to the mesocoms without addition of dust has been observed. A simple 1-D model of the mesocosm demonstrated that during the experiment the addition of dust was a sink rather than a source of Fe due to the scavenging on dust particles (Ye et al., 2010).

2. Additionally batch experiments performed with filtered seawater of the corresponding mesocosm and a second addition of simulated aeolian dust showed a clear increase in the Fe solubility capacity with the seawater which was taken 168 h after the first seeding. Wagener et al. (2010) postulated that the dust addition could have induced the production of Fe-binding ligands and therefore increased significantly the solubility capacity of Fe. This would imply that a second addition of dust to the mesocosms might have a stimulatory effect on Fe dissolution and a contrasting impact than the first addition.

A second experimental campaign was performed in June and July 2010 (DUNE-2) (Guieu et al., 2012). Based on the experience gained during the DUNE-1 experiment, the strategy for studying trace metals was slightly changed. During DUNE-1, Fe budget calculations over the entire experiment have shown that an important amount of Fe was not recovered, which might be due to an insufficient vertical and temporal resolution of sampling. In order to evaluate the impact of the vertical sampling resolution on the inventories estimation, in two of the mesocosms amended with dust (DUST-Mesos) sampling in 2010 was performed with a higher vertical resolution with six (0.2, 2.5, 5, 7.5, 10 and 12.5 m) instead of only three depths (0.2, 5 and 10 m). Moreover, additionally to dFe, two more dissolved trace metals have been examined in the course of DUNE-2: the biogeochemically important micronutrient Manganese (dMn) and the crustal metal Aluminium (dAl). In contrast to dFe, there is no organic speciation known for dAl and it is also considered to be negligible for dMn (Roitz and Bruland, 1997; Sañudo-Wilhelmy et al., 1996). Al is a major and relatively invariant component of the earth crust and dAl is not known to be actively assimilated by organisms. However, dAl is strongly influenced by scavenging mechanisms and is therefore considered as a potentially useful tracer for lithogenic input on relatively short time scales due to its important scavenging on particles (Dammshäuser et al., 2011). On the other hand, Mn is a bioactive metal with a complex chemistry in seawater: while Mn(II) is not thought to be organically complexed, dissolved Mn(III) and Mn(IV) organic species are possible, but have not yet been observed in oxygenated seawater. Another important difference

compared to DUNE-1 is that DUNE-2 was carried out with two consecutive seedings with the same amount of simulated dust. The changes after each addition were followed for one week allowing to asses if the biogeochemical response to a second seeding can be influenced by the response to the former seeding.

5 This paper illustrates the dissolved trace metal stocks during the DUNE-2 experiment and based on the revised experimental strategy, the specific objectives of this study are:

1. Using the inventories of the three different dissolved trace metals in the surface waters, and the differences in removal of dFe and dMn in contrast to dAl, the scavenging and/or biological utilization versus dust dissolution from the dust seeding 10 might be evaluated on different time scales.

2. Furthermore, the loss rates of the three dissolved trace metals in the DUST-Mesos can be calculated. This knowledge of loss rates is highly novel and will finally enable a precise quantification of the processes occurring after the dust seeding.

2 Materials and methods

15 2.1 Experimental design and sampling

The DUNE-2 mesocosm experiment design is based on the exact same protocol as described in detail earlier (Guieu et al., 2010a) for the DUNE-1 experiment in 2008 (Guieu et al., 2012). In summary: in June 2010, seven trace metal clean mesocosms were deployed in the bay of Elbo in the preservation area of Scandola near Corsica (42.374° N, 20 8.554° E) during typical oligotrophic summer conditions (Millot, 1999). The mesocosms were purely made out of plastic and were composed of a cylindrical section of 12 m length and 2.3 m of diameter. The conical bottom started at 12 m depth and ended with a sediment trap at 14.5 m depth. In each mesocosm, the total seawater volume was 52 m^3 and the water column was preserved. To protect the mesocosms against natural 25 occurring dust events, they were covered with a transparent cover which was designed

to let natural light pass and to allow gas exchanges between the water body and the atmosphere. The three mesocosms to which the dust was added are referred to here as D1, D2 and D3, hereafter referred to as "DUST-Mesos". Further three trace-metal clean mesocosms were kept without seeding as the "CONTROL-Mesos" (labeled here C1, C2 and C3). For comparison between the "CONTROL-Mesos" and the environment, samples were also taken outside the mesocosms (hereafter labeled as OUT).

After deploying the mesocosms, they were left open for 24 h in order to let the water masses settle and after closing the mesocosms, sampling was performed to determine the initial conditions. Two consecutive seedings with cloud processed dust were performed at an interval of one week. Each seeding was followed for a week with a high resolution sampling in the first 24 h and subsequent daily sampling. Therefore DUNE-2 had a higher time resolution than DUNE-1 where sampling was performed daily for most parameters (Guieu et al., 2010b). The first seeding with dust took place at t0, the second after 166 h. The seedings with 41.5 g of artificial dust to the surface of the mesocosms correspond to a realistic, high wet deposition of $10\,\mathrm{g\,m^{-2}}$.

In each of the six sample mesocoms flexible reinforced PVC tubings were installed at 0.2, 5 and 10 m depth. Sampling for dissolved trace metals was conducted using 0.2 μm Sartobran filter cartridges (Sartorius, Germany) adapted to a Teflon^{TM} diaphragm pumping system and then the samples were directly collected into the corresponding bottles. Additionally to DUNE-1, two mesocosms were deployed with three supplementary tubings installed at 2.5, 7.5 and 12.5 m depth, in order to improve the resolution in the water body and to be able to follow the processes after a simulated dust storm on a smaller scale. The additional tubings were installed in D1 and D2, two of the three mesocosms that were fertilized with artificial dust (see below).

2.2 Chemical analysis

2.2.1 Reagents and bottles

To avoid contamination in this study, strict attention was given to control the poten-
tial risks. All manipulations were performed in class 100-laminar flow benches. All
5 reagents that were used were of highest purity available (Fischer Scientific and Sigma-
Aldrich) and were prepared using deionized ($18\,\mathrm{M\Omega\,cm^{-1}}$ resistivity) water (MQ water)
from a Milli-Q purification system (Millipore). Sub-boiled quartz-distilled hydrochloric
acid (hereafter Q-HCl) was made by single distillation from 25 % HCl. All plasticware
and bottles (low density high polyethylene (LDPE) and Polytetrafluoroethylene (PTFE))
10 used for acidified seawater samples for the total trace metal analysis were cleaned ac-
cording to the trace metal clean procedures (Bruland et al., 1979; Cutter et al., 2010)
and then protected by double bags (Minigrip[TM]). The filtered samples for dissolved
trace metal analysis were directly acidified on-land with Q-HCl to pH < 2, for dMn, e.g.
to pH 1.7, under a class 100-laminar flow bench. Sample processing and analysis steps
15 were performed in laminar flow benches inside class 100 clean rooms in Kiel and in
Villefranche sur Mer.

2.2.2 Dissolved manganese analysis

Samples for dissolved manganese (dMn) were analyzed on site. The acidified samples
were spectrophotometrically analyzed using a slightly modified flow-injection analy-
20 sis system (FIA) built after (Aguilar-Islas et al., 2006). Briefly we used one 8-channel
peristaltic pump (Rainin), two electronically actuated 6-port valves, one electronically
actuated 10-port sample valve (all VICI, Valco Instruments), one dry bath (Fisher) kept
at 35 °C and a variable wavelength spectrophotometer (USB-4000, Ocean Optics, Inc.)
with an internal Ocean-Optics light-source and a 1 cm quartz flow-through cell (100-QS,
25 10.00 mm, Hellma GmbH & Co. KG). The flow rates were identical with those in Aguilar-
Islas et al. (2006). The pre-concentration column (GLOBAL-FIA), filled with Toyopearl

AF-Chelate-650M resin, was preconditioned for 30 s by flushing with $0.05\,\mathrm{mol\,l^{-1}}$ ammonium borate rinse solution. The timing parameters were for preconditioning, loading, rinse and elution of the column: 30, 120, 30, 180 s.

The calibration curves, for this recently setup method in our group, were determined daily by the addition of standards (0–$10\,\mathrm{nmol\,l^{-1}}$) produced by serial dilution of a 1000 ppm Mn^{2+} standard (Fluka) into 0.2 µm filtered Mediterranean seawater (R1; t0; Out; 5 m). For external validation, selected samples were also analyzed in the clean laboratory in Kiel by graphite furnace atomic absorption (ETAAS, Perkin-Elmer Model 4100ZL).

Samples, standard additions and blanks were measured in triplicates. Analytical precision (expressed as percent relative standard deviation) was typically $< 8\,\%$ at $3.6\,\mathrm{nmol\,l^{-1}}$ under the conditions employed here. The accuracy of the analytical procedure was evaluated by daily measurements of SAFe intercalibration samples S and D2. It should be noted however that the SAFe concentrations are over a lower range ($> 1\,\mathrm{nmol\,l^{-1}}$) than the seawater samples from the mesoscoms ($< 3.5\,\mathrm{nmol\,l^{-1}}$) which lead to lower precision for the SAFE samples using our system optimized for Mediterranean surface waters. SAFe values determined while in Corsica were as follows: $0.85 \pm 0.14\,\mathrm{nmol\,l^{-1}}$ (S) and $0.35 \pm 0.09\,\mathrm{nmol\,l^{-1}}$ (D2) of dMn ($n = 8$) (consensus values are $0.79 \pm 0.06\,\mathrm{nmol\,l^{-1}}$ and $0.35 \pm 0.06\,\mathrm{nmol\,l^{-1}}$, respectively). We used a large volume of secondary standard (0.2 µm filtered Mediterranean seawater (R1, t0, Out, 5 m)) throughout this work as the seawater in which standard additions were prepared, the complete Mn-FIA measurements over the course of the work in Corsica resulting in a value of $3.60 \pm 0.30\,\mathrm{nmol\,l^{-1}}$, which was in good agreement with values measured by ETAAS in Kiel: $3.55 \pm 0.08\,\mathrm{nmol\,l^{-1}}$. The detection limit ($3\sigma$ of the blank) for the Mn flow injection system used here was estimated in the lab in Kiel by repeated measurements of low Mn Antarctic seawater ($< 0.2\,\mathrm{nmol\,l^{-1}}$; collected during ANTXXIV-3) at $150\,\mathrm{pmol\,l^{-1}}$. The use of a low Mn or Mn free seawater is preferred to running MQ blanks as both in Corsica and in Kiel, we found that there was detectable Mn in the MQ systems due to problems with the ion-exchange units of the systems.

2.2.3 Dissolved iron analysis

dFe concentrations were analyzed at Laboratoire d'océanographie de Villefranche sur Mer between 4 and 10 months after the experiment. A flow injection system with online preconcentration and chemiluminescence detection was used as described in Bonnet and Guieu (2006). The detection limit (DL) was $25\,\mathrm{pmol\,l^{-1}}$ on average and blanks were between 50 and $150\,\mathrm{pmol\,l^{-1}}$. An internal acidified seawater standard was measured in order to control the stability of the analysis during each series of measurements. The reliability of the method was controlled by analyzing the D2 SAFE seawater standard (Johnson et al., 2007) which was determined as $0.84 \pm 0.04\,\mathrm{nmol\,l^{-1}}$ of dFe ($n = 5$) (consensus value is $0.90 \pm 0.02\,\mathrm{nmol\,l^{-1}}$).

2.2.4 Dissolved aluminium analysis

The Aluminium analysis was conducted in GEOMAR, Kiel a few month after the experiment using the fluorometric method described by (Hydes and Liss, 1976). In short, the reagent lumogallion is added to the sample, which is then buffered to pH 5 with ammonium-acetate, and heated to 40–$50\,°C$ for $3\,h$ to accelerate complex formation. The fluorescence of the sample was measured with a Hitachi FL 2700 Fluorescence Spectrophotometer (excitation wavelength $497\,\mathrm{nm}$, emission wavelength $572\,\mathrm{nm}$). The detection limit varied between 0.1 and $0.3\,\mathrm{nmol\,l^{-1}}$, the blank values between 0.4 and $0.6\,\mathrm{nmol\,l^{-1}}$ for the different days of analysis. In the SAFe reference seawater S1 (S1 543, S1 474) $1.81 \pm 0.24\,\mathrm{nmol\,l^{-1}}$ of Al ($n = 4$) were determined (consensus value is $1.74 \pm 0.09\,\mathrm{nmol\,l^{-1}}$).

2.2.5 Other dissolved total trace metal analysis

Dissolved total trace metal (Cadmium (Cd), Cobalt (Co), Copper (Cu), Nickel (Ni), Plumb (Pb) and Zinc (Zn)) concentrations were determined in the clean laboratory of the GEOMAR in Kiel using the graphite furnace atomic absorption

(ETAAS, Perkin-Elmer Model 4100ZL) method after pre-concentration by simultaneous dithiocarbamate-freon extraction from seawater (100–250 g) (Grasshoff et al., 1983; Danielsson et al., 1978). Note that the samples were not UV irradiated prior to analysis, recent work has shown that this is important for determining total Co concentrations
5 (Shelley et al., 2010; Milne et al., 2010). The accuracy of the method was evaluated by measuring SAFe and GEOTRACES intercalibration samples.

A few samples for dissolved Mn, as a comparison to the direct analysis on Corsica, were analyzed by graphite furnace atomic absorption (ETAAS, Perkin-Elmer Model 4100ZL) in the clean laboratory in Kiel after solvent extraction modified after (Klinkham-
10 mer, 1980). SAFe reference seawater D1 was determined as 0.423 ± 0.05 nmol l^{-1} (consensus value (0.35 ± 0.06 nmol l^{-1}) and are given in the Supplement.

3 Results

The complete set of data is available as Supplement to this paper.

The nomenclature for samples of the DUNE-2 experiment is as following: "Rx-D (or
15 C or OUT)y-zz". x corresponds to the number of the cast , y corresponds to the mesocosm number ("Cy" for the CONTROL-Mesos, "Dy" for the DUST-Mesos and "OUT" for outside the mesocosms) and zz corresponds to the sampling depth in meters. To each cast corresponds a time tx expressed in hours (x) since the first dust addition. The concentrations OUTside the mesocosms are not reported in the figures, but are
20 available in the Supplement.

3.1 Evolution of dissolved manganese (dMn)

Figure 1 shows the evolution of the concentration of dMn as a function of time after the first seeding and depth in each of the mesocoms. The initial dMn concentrations OUTside and in the CONTROL- and DUST-Mesos were 3.4 ± 0.6 nmol l^{-1}. Directly in the first
25 23 h after the first dust addition, the dMn concentrations increased by 1.5–1.8 nmol l^{-1}

in the surface and at mid-depth (D1 and D2). In D3 no samples were taken 23 h after the first addition, but afterwards a similar trend to D1 and D2 was seen with a continuation of the increase in dMn most pronounced in the surface. After the continuous increase since the first seeding with dust, at t71h dMn reached its maximum in all three DUST-Mesos and in D1 at 5 m depth the concentration was as elevated as 7.2 nmol l^{-1}. After this initial elevation of dMn, overall the concentration then decreased slowly in all three mesocosms with time down to 3.0–4.6 nmol l^{-1} after a week. These values were in the range of the values before the first addition with dust.

After the second dust addition to the surface of the DUST-Mesos, the increase in dMn was more pronounced than after the first addition. Concentrations of dMn in the surface (0.2 m) after 5 h (t171) and 9 h (t175) increased to 13.2 nmol l^{-1} and 11 nmol l^{-1} for D2, to 9.8 nmol l^{-1} and 9.2 nmol l^{-1} for D1 and to 7.8 nmol l^{-1} and 8.6 nmol l^{-1} for D3. In these first 24 h after the second dust addition the concentrations of dMn at 5 m and 10 m remained constant at 3.2 to 4.4 nmol l^{-1}. While the values in the surface decreased slowly after the first strong pulse following the second addition, the dMn values increased at 5 m after 24 h and even more after 48 h. At all depths the dMn concentrations in the DUST-Mesos decreased again with time down to 3–5 nmol l^{-1} after 5 days (with the exception of D3 10 m with a dMn concentration of 5.7 nmol l^{-1}).

3.2 Evolution of dissolved iron concentration (dFe)

In Fig. 2, the evolution of dFe values in the CONTROL- and DUST-Mesos are shown. The initial dFe values before the dust addition varied between 2.2 and 4.4 nmol l^{-1} inside the mesocoms and outside (OUT, values available in the Supplement). After the first addition of dust (R2, t10), there was a direct decrease in the dFe concentrations to 2.5–2.9 nmol l^{-1} in the surface of the DUST-mesoss and as low values as 1.5 nmol l^{-1} were measured in D2 and D3. 23 h after the first dust addition the values inside the CONTROL-Mesos still ranged from 3.0 to 3.5 nmol l^{-1}. With more time elapsing, this decrease in the dFe concentrations continued in the DUST-Mesos but also occurred in

the CONTROL-Mesos and "OUT". After 143 h the dFe values in the CONTROL-Mesos varied from 1.4–2.1 nmol l^{-1} and in the DUST-Mesos from 1.6–2.0 nmol l^{-1}.

After the second dust addition, a significant increase in dFe was observed in the DUST-Meso, whereas dFe values remained constant in CONTROL-Mesos. Directly after this addition there was a strong increase in the surface with a maximum at 25 h (t191) after the second dust addition. In D1 and D2, the dFe concentration increased up to 6.1 nmol l^{-1} at 2.5 m and up to 3.8 nmol l^{-1} in the surface of D3. In the first 24 h after the second addition the dFe values had increased in all the DUST-Meso. However after 49 h (t215), the dFe concentrations already decreased quickly again down to 1–1.8 nmol l^{-1}. This range remained the same until the end of the experiment.

3.3 Evolution of dissolved aluminium (dAl)

The evolution of the concentrations of dAl is displayed in Fig. 3. In all three CONTROL-Mesos, similar features were observed: the values decreased nearly linearly with time over the two weeks of the experiments, from 44 nmol l^{-1} to 38 nmol l^{-1}. Values from outside the mesocoms ("OUT") were in the same range as those in the CONTROL-Mesos.

In the DUST-Mesos, directly after the first addition of dust (10 h), the surface dAl values increased to 54 nmol l^{-1} and the rest of the water column was also elevated (48–50 nmol l^{-1}). The increase continued throughout the DUST-Mesos (50–56 nmol l^{-1}), but most distinctive in the surface with concentrations up to 60–63 nmol l^{-1} after 47 h. At the end of the first dust addition the dAl concentrations were pretty uniform in all DUST-Mesos at approximately 55 nmol l^{-1}.

After the second dust addition the dAl concentrations increased by approximately 10 nmol l^{-1} after 49 h (t215), for example up to 78 nmol l^{-1} in the surface in D1. 73 h after the second seeding (t239), the minimum value was 58 nmol l^{-1} and the maximum was reached with 66 nmol l^{-1} at several depths. In the end of the experiment, the values decreased to 53 nmol l^{-1} in D1 and 55–60 nmol l^{-1} in D2. In D3, a similar decrease with time could be observed, but the initial increase after the second addition was smaller

compared to D1 and D2. In the end of the experiment (t311), the values dropped to 42–46 nmol l^{-1}.

3.4 Total dissolved trace metal concentration analysis

Samples for total dissolved trace metal concentrations of Cd, Co, Cu, Ni, Pb and Zn were measured at 5 m depth at R1, R8 and R16 and the values are given in Table 1. For most of the total dissolved trace metals no significant change at the three points (start, before the second addition and end) sampled are observed.

Indeed dissolved Cobalt (dCo) that showed initial concentrations of 0.09–0.10 nmol l^{-1}. At t143h (R8) the dCo concentrations did not change in C2, C3 and D1, but increased to 0.12 nmol l^{-1} in the other mesocoms and OUT. This trend continued and in the end the dCo concentrations increased to 0.14 nmol l^{-1} in the CONTROL-Mesos and OUT. In the DUST-Mesos dCo reached 0.17 ± 0.02 nmol l^{-1}.

4 Discussion

4.1 Trace metal concentrations at the DUNE site

The average values of the total dissolved trace metal concentrations ($\pm$ standard deviation) before the addition of dust at 5 m depths at the DUNE site are given in Table 2. For all the trace metals measured during DUNE-2, no significant differences could be observed between the initial values OUT- and inside the mesocosms. This indicates that the deployment protocol of the mesocoms, developed for the DUNE experiment (Guieu et al., 2010a), does not contaminate the water column trapped inside for the nine trace element measured in this study. This is agreement with the results obtained for Fe during DUNE-1 (Wagener et al., 2010).

All the total trace metal concentrations measured at the DUNE sampling site before the seeding are representative for the Western Mediterranean Basin (Boyle et al., 1985;

Copin-Montegut et al., 1986; Kremling and Petersen, 1981; Morley et al., 1997; Sherrell and Boyle, 1988; Yoon et al., 1999).

Sherrell and Boyle (1988) reported maximum values in the core of the Atlantic inflow jet in the Strait of Gibraltar with concentrations of 9.4 nmol kg^{-1} of total dissolved Zinc (dZn) and 53.0 nmol kg^{-1} of Fe. However these high values can be explained by the rise of the Cd, Cu, Fe, Mn and Zn concentrations by a factor of 2–7 due to river discharge (acid mine drainage) (Elbaz-Poulichet et al., 2001). Reported surface Zn values by Sherrell and Boyle (1988) were in agreement with our measured values ranging from 1.0 to 3.5 nmol kg^{-1}. Another study of dMn concentrations in the Mediterranean also showed a surface enrichment up to 4.19 nmol l^{-1} (Statham et al., 1985). The range of reported dFe concentrations is similar to previously published ones in the Western Mediterranean Basin (Bonnet and Guieu, 2004; Sarthou and Jeandel, 2001; van den Berg, 1995). However, the dFe start values in the mesocosms were clearly increased compared to other surface oceans at the same latitude (e.g. the Pacific, Buck et al., 2006). These high dFe start values might have resulted from a previous natural dust event or from runoff from land due to heavy rains before the start of the experiment as postulated for the DUNE-1 experiment (Wagener et al., 2010). Our observed dAl concentrations are in the same range as previously reported surface values of about 56 nmol l^{-1} close to our study site off the coast of Corsica in 1977 (Caschetto and Wollast, 1979). Similar dAl concentrations have also been observed in the Western Mediterranean Basin (Chou and Wollast, 1997; Hydes et al., 1988; van den Berg et al., 1994).

4.2 Effect of the temporal and vertical resolution on the determination of the trace metals inventories

Mesocosms are closed systems without lateral advection. Therefore after the addition of dust, its effect on the cycling of trace metals can be completely assessed by using inventories over the water column of the mesocosms. For this reason, in the two

following sections the discussion will be based on inventories estimated as described in the following paragraph:

For the three main dissolved trace metal measured in all mesocosms, the inventories were calculated for each 2.5 m depth layer (0–2.5, 2.5–5, 5–7.5, 7.5–10 and 10–12.5 m). The final conical section of the mesocosms was neglected. Missing values were interpolated if necessary: the average values were used between two depths, or the closest value was used for the extreme values. The inventories for the 2.5 m increments were then added up as an inventory for the corresponding mesocosm at the corresponding time point tx.

The DUNE-1 experiment has demonstrated that variations in concentrations of elements delivered by dust (Fe and P) can only be observed during a short time span (h) after the addition of dust and on small spatial scales (meter in vertical) (Pulido-Villena et al., 2010; Wagener et al., 2010). Therefore the question of the vertical and temporal resolution of the sampling is crucial for inventory calculations and our strategy during DUNE-2 was well adapted to this issue. In Fig. 4, inventories for dAl and dFe in the mesocosms D1 and D2, which were equipped with 6 sampling depth, are presented as a function of time. These inventories were calculated with samples every 2.5 m (high resolution), 5 m (normal resolution) and at only 1 depth (low resolution).

It can be clearly seen in Fig. 4, that in the first 24 h after the second dust addition, dFe inventories show differences of more than 50 % between the high and the low resolution and of approx. 20 % between the normal and the low resolution. This implies that in this initial time period after the seeding, when processes at the surface of the particles can be restricted to the upper few meters of the mesocosms, a high vertical resolution is necessary for the detailed description of the fate of the dust particles in the mesocosms. However, considering the rest of the experiment for both elements, the differences in the inventories between the high and the normal resolution are remarkably lower with less than 5 %. Figure 4 also illustrates that a lower than daily sampling frequency would not have captured some of the trace metal changes induced by the dust addition in the first 48 h.

This implies two main issues for the discussion of trace metals changes after the addition of dust: (1) a high temporal resolution is necessary to catch features in the first 48 h of the experiment. For this reason most of the trace metals that have only been sampled every 8 days cannot be discussed in regard to the dust particle additions, because the most relevant variations could not be observed. (2) High vertical resolution changes the inventories only during these first hours after the seeding. For this reason, inventories calculated with the normal resolution (0, 5 and 10 m) are sufficient to describe most of the variations observed.

4.3 Changes in trace metal inventories: dissolution and scavenging after the seeding

In Fig. 5a, the calculated temperature difference between the surface and the bottom of the mesocosm is plotted as the only available physical continuously measured parameter. The temperature difference between 0 and 10 m measured inside the mesocosm is used as a proxy for mixing or stratification in the mesocosm in order to discuss the changes in the inventories within the mesocosms. The main feature this proxy provides is that the course of the experiment can be separated into four periods: a relatively well-mixed mesocosm during the first 96 h of the experiment, followed by a stratification of the water column (96–180 h). The second addition of dust therefore occurred in a more stratified water column than the first one. After t180 the water column was mixed again until 240 h when a new stratification followed until the end of the experiment (Guieu et al., 2012).

Figure 5 shows the evolution of the dMn (B), dFe (C) and dAl (D) inventories as a function of the time since the addition of dust. The plotted inventories were calculated as arithmetical means for the CONTROL- and the DUST-Mesos. The major observed trends were: for all three elements (Fe, Al and Mn), the inventories in the DUST- and CONTROL-Mesos were equivalent before the start of the experiment. The dMn and dAl DUST-inventories were always higher than the CONTROL-inventories with similar trends observed: dMn and dAl CONTROL-inventories remained constant or decreased

slightly throughout the whole experiment, whereas the inventories in the DUST-Mesos showed a remarkable increase during 48–72 h after the seedings, followed then by a decrease in the inventories in the following days. dFe inventories showed a different trend with a distinct decrease in the DUST- and CONTROL-Mesos after the first dust

5 seeding. This decrease until 72 h was followed by constant inventories during the rest of the experiment. Only a very transient increase could be observed in the DUST-Mesos 24 h after the second addition of dust.

Based on these inventory calculations, changes are discussed (1) in terms of absolute inventories based on estimations of trace metal solubilities from dust particles and

10 (2) in terms of relative changes of the inventories based on estimations of dissolution and loss rates of the three elements.

4.3.1 Estimation of dissolution during the mesocosm experiment

The fractional solubility of an element from dust particles in seawater (Baker and Croot, 2010) is commonly expressed as the percentage of the soluble element compared

15 to the total element in the dust particle. This percentage allows an estimation of the impact of the atmospheric particle flux on the dissolved (and bioavailable) stock in the ocean (Landing and Paytan, 2010). In recent years, two major experimental protocols have been used to assess the solubility of collected dust particles in seawater: flow through protocols (e.g. Buck et al., 2006) and batch experiments (e.g. Bonnet and

20 Guieu, 2004). As discussed in Wagener et al. (2010), mesocosms allow us to estimate solubility from dust particles in a much more realistic and in situ way: the settling of the particles through the water column and interactions with naturally occurring particles are both integrated in this approach. To estimate the solubility of an element in the added dust, the time point when the inventory is at its maximum after the addition of

25 dust has to be used. At this time point the amount of the dissolved element added to the seawater by dust, is approached as the difference between the inventories in the DUST- and the CONTROL-Mesos. This elemental stock is divided by the percentage of each element added with dust in order to evaluate the percentage of dissolution.

Title Page

Abstract | Introduction

Conclusions | References

Tables | Figures

◄ | ►

◄ | ►

Back | Close

Full Screen / Esc

Printer-friendly Version

Interactive Discussion

In addition to the consideration of the mesocosm as a completely closed system, it is assumed that the resolution is important enough to achieve correct inventories. This estimation was made for each dust addition even if the inventory had not reached the CONTROL-Mesos value again after the first addition. Values of fractional solubility are reported in Table 3.

The fractional solubility for Al after the first and second dust addition was, respectively 0.84 % and 1.86 %. The difference between both additions is due to the fact that the inventories in the DUST-Mesos had not decreased back values comparable to the CONTROL-Mesos after the first addition. Using the Al inventory in the DUST-Mesos before the second seeding as a baseline would give a fractional solubility for Al of 0.74 % which is very similar to the value after the first dust addition. Fractional Al solubilities of 0.087 to 14.3 % (average 4.6 %) in seawater with aerosol samples collected at Hawaii were reported by Measures et al. (2010) and for Saharan dust fractional Al solubilities of 1.9–5.5 % in pH 4.7 solutions have been published by Baker et al. (2006). For Mn, after both dust additions the fractional solubilities are in the same order of magnitude with values of 40 and 45 %. In literature, Mendez et al. (2010) reported values of 12 to 14 % with Saharan dust in seawater, Baker et al. (2006) reported values of 50–64 % in pH 4.7 solutions and Guieu et al. (1994) have shown fractional Mn solubilities of 30–35 % in pH 7 solutions. Values obtained with the "mesocosm" method are thus comparable to other experimental set-ups.

During the DUNE-1 experiment no dissolution from the dust particles was observed for Fe and therefore no value for the fractional solubility of Fe was obtainable (Wagener et al., 2010). Here, during DUNE-2, the same result was obtained after the first seeding, but a fractional solubility of 0.12 % was estimated after the second addition of dust. The reasons for this change in fractional solubility are discussed in Sect. 4.5. Literature values for fractional Fe solubility spread over more than three orders of magnitude (Baker and Croot, 2010) with large differences depending on atmospheric and marine processes as well as on the experimental design used. In summary, based on a much more realistic protocol than the commonly used laboratory protocols, the fractional

Impacts of dust deposition on dissolved trace metal concentrations

K. Wuttig et al.

Title Page

Abstract	Introduction
Conclusions	References
Tables	Figures

◀◀   ▶▶

◀   ▶

Back   Close

Full Screen / Esc

Printer-friendly Version

Interactive Discussion

solubility of Mn and the fractional solubility of Al in dust are in the range of previously published values. This overall gives more confidence in consensus ranges for fractional Al and Mn solubility from dust. For Fe, the complex processes that control the fractional solubility are clearly shown here, and indicate that the use of an absolute value for the
⁵ fractional solubility of Fe is not realistic.

4.3.2 Dissolution and scavenging rates

The rates of the decreases or increases of the inventories were quantified by estimating loss and dissolution rates. These estimated rates for dMn, dAl and dFe are reported in Table 4.
¹⁰ An overall trend, observed for the three dissolved trace metals, was a general decrease in the inventories in the CONTROL-Mesos with low loss rates. This could correspond to scavenging on particles which is a common physico-chemical process occurring in the ocean for trace metals (Turekian, 1977). The loss rate was well defined for Al, which is not known to have a bioactive role, whereas some variations over the gen-
¹⁵ eral decreasing trend were observed for dFe and dMn. This might be due to changes in biological utilization in response to the changes in stratification in the mesocosms.
In the DUST-Mesos, the inventories of dMn and dAl increased with dissolution rates which were quite similar for both dust additions. It is interesting to notice, that even if the dust additions occurred in different stratification conditions (Fig. 5a), the increase in
²⁰ the inventories and the dissolution rates were the same when integrated over the entire mesocosm. In contrast to this finding, Fig. 1 clearly shows that the increase in dMn concentrations was occurring over much more of the water column for the first compared to the second seeding, in which the increase was concentrated in the first few meters of the mesocosms. This implied that the overall rate of dissolution seemed not to be
²⁵ affected by the mixing of the water column, but the dilution of the dissolved elements was changed. This has important implications on the importance of the resolution of the sampling in order to estimate the impact of a dust addition.

Title Page

Abstract | Introduction

Conclusions | References

Tables | Figures

◄ | ►

◄ | ►

Back | Close

Full Screen / Esc

Printer-friendly Version

Interactive Discussion

The loss rates of dAl and dMn behaved differently. dMn showed quite equivalent loss rates for the first and the second seeding, whereas the dAl loss rate was one order of magnitude higher after the second seeding ($-1.9\,\mu mol\,m^{-2}\,h^{-1}$) in comparison to the time after the first one ($-0.07\,\mu mol\,m^{-2}\,h^{-1}$). Scavenging of dAl is sensitive to the amount of biogenic particles (Moran and Moore, 1988) in seawater. During DUNE-2, an increase of chlorophyll a in the DUST-Mesos is reported by Ridame et al. (2012), suggesting an increase of biomass, and this could explain the observed significant change in the loss rates for dAl. Correlations of dAl and chlorophyll a were also found by Moran and Moore (1988). However, this is not observed for dMn which had similar loss rate after the first and the second addition of dust, indicating that dMn was not appreciably lost by scavenging on biogenic particles.

Changes in the dFe inventories were complex in regard to the dust addition. In the first 24 h, the loss rate in the DUST-Meso was $-0.23\,\mu mol\,m^{-2}\,h^{-1}$, whereas it was slightly positive in the first 24 h in the CONTROL-Mesos and the inventories only started to decrease after 24 h. The loss rate in the DUST-Mesos in the first 24 h was comparable to the one reported for DUNE-1. This might demonstrate a contrastable scavenging onto dust particles, which had been demonstrated for DUNE-1 (Wagener et al., 2010). In the first 72 h an overall sharp decrease in the loss rates was observed in both the CONTROL- and the DUST-Mesos. This decrease had not been observed in the CONTROL-Mesos during DUNE-1. A plausible reason for this decrease could be adsorptions onto the mesocosms plastic walls. It has been demonstrated in bottle experiments (e.g. Fischer et al., 2007), that this could represent up to 50 % of dFe in bottles. But, as the surface to volume ratio is much lower for large mesocosms, wall adsorption can certainly not explain entirely the Fe loss in the CONTROL-Mesos.

After the second addition, a transient dissolution of Fe was observed within 24 h with a dissolution rate of $0.70\,\mu mol\,m^{-2}\,h^{-1}$, which was higher than the loss rate observed after the first seeding. Wagener et al. (2010) estimated a biological uptake of dFe in the mesocosms of 0.02 to $0.04\,\mu mol\,m^{-2}\,h^{-1}$. This dissolution from dust particles could therefore sustain biological activity in the case of a Fe limitation.

Title Page

Abstract | Introduction

Conclusions | References

Tables | Figures

◄ | ►|

◄ | ►

Back | Close

Full Screen / Esc

Printer-friendly Version

Interactive Discussion

4.4 Insights into the time scales and possible mechanisms of dissolution and scavenging processes during a dust event

Our unique dataset allows a first order look at the scavenging mechanisms following atmospheric deposition events. Previous work on this has been done over much larger temporal (week to month) and vertical (hundreds of meters) scales through the use of sediment traps (Brust et al., 2011; Brust and Waniek, 2010). The DUNE-2 experiment is unique in the sense that optical measurements in the water column were made simultaneously allowing an assessment of the particle residence time. This particulate export was controlled partly by the formation of organic-mineral aggregates (Bressac et al., 2012a). The mass of material exported into the sediment traps (collected every 24 h) was the highest at t48. At the end of the first seeding experiment, the optical parameters were homogenous from 0 to 10 m depth, but still slightly higher than before the first addition of dust (Bressac et al., 2012a). During the second part of the DUNE-2 experiment, optical measurements were also performed in order to follow the particle dynamic (Bressac et al., 2012b). These optical measurements revealed an accumulation of particles in the upper 2.5 m layer directly following the second dust addition likely due to the stratification of the water column (Fig. 4a). This higher residence time of particles in the subsurface could explain the high Fe dissolution observed after the second addition of dust. However, the mass of material exported into the sediment traps was the highest at t24. Indeed, the mixing of the water column occurred between t13 (maximum of the temperature difference, 0–10 m) and t48 (Fig. 4a). Simultaneously, a sudden decrease of the beam attenuation in the subsurface was observed between t8 and t25 revealing the activation of the particulate export (Bressac et al., 2012b).

The optical measurements indicate that part of the Saharan dust was lost from the mixed layer rapidly (estimated sinking rates ~ 24–$86\,\mathrm{m\,day^{-1}}$) and that the particulate export following the simulated dust event was a nonlinear multi-step process. As reported above, after the first seeding with dust, part of the Saharan dust pool was rapidly exported. The physical characteristics of the water column differed widely between both

dust addition experiments. This difference in physical conditions, especially marked during the first hours after the seedings, likely impacted the particulate export dynamic and could partly explain the differences observed in the kinetic dissolution between the two additions of dust. These findings are important in the present context as they represent the removal of particulate metals and the adsorbed or scavenged metals they contain. Our observations are consistent with field studies from the Atlantic Ocean which have shown that the residence time of dFe in surface waters is strongly influenced by Saharan dust deposition (Croot et al., 2004), while that of Mn and Al are much less so (Jickells et al., 1994; Jickells, 1999). Earlier laboratory studies have shown that scavenging and export are controlled by the formation of organic-mineral aggregates (Balistrieri et al., 1981; Hunter, 1983) with scavenging related to particle concentration (Honeyman et al., 1988). For particle reactive elements, e.g. Fe, the transfer of colloidal to particulate phases (colloidal pumping) is also important (Honeyman and Santschi, 1991). Combining the optical data with the dissolved trace metal data suggests that the larger dust particles sunk out quickly but played a small role in scavenging Mn and Al from the water column, as release processes dominated at that time. Thus scavenging by smaller particles (dust and phytoplankton/bacteria) appears to be the more important removal term over the duration of the experiment. In particular the production of organic material by bacteria and phytoplankton would lead to increased formation of organic-mineral aggregates and lead to increased scavenging.

4.5 Effect of two successive dust additions on the biogeochemistry of trace metals

During the DUNE-1-P experiment, batch reactor dissolution experiments of dust performed with filtered seawater collected in the DUST- and CONTROL-Mesos have shown that the solubility capacity of Fe increased significantly in the DUST-Mesos 7 d after the addition of dust (Wagener et al., 2010). A probable mechanism could be the production of specific Febinding ligands by heterotrophic bacteria in the DUST-Mesos in response to a change in the bioavailability of Fe after the settling of particles. This

hypothesis was supported by observations of changes in the diversity of the bacterial community attached to the dust particles (Laghdass et al., 2011).

Here during DUNE-2, this hypothesis was completely verified for dFe where a comparable response to the first addition of dust was observed with an increased scavenging of Fe, whereas after the second addition of dust dissolution of Fe from the dust particles was observed. No additional dust dissolution Batch reactor experiments were performed during DUNE-2, but Fe-binding ligand measurements by ligand competition and cathodic stripping voltammetry (Croot and Johansson, 2000) showed a significant increase of Fe-binding ligands 144 h after the first seeding with dust (Wagener et al., 2012).

A different behavior of Mn and Al in comparison to Fe was observed and can be explained by their different speciations in seawater. Whereas the solubility of Mn and Al is controlled solely by inorganic species, the solubility of soluble and colloidal Fe is controlled by organic complexes (Gledhill and Buck, 2012). Indeed, an opposite effect was observed for dAl than for dFe. The consecutive additions of dust did not impact the dissolution of Al but the loss rate through the increase of scavenging on biogenic particles induced by biomass increase consecutive to the first dust addition. However, this mechanism was not observed for Mn which is certainly subject to more complex redox and photochemical processes (Sunda and Huntsman, 1987, 1988). Overall this demonstrates that the quantification of the effect of a dust event on the biogeochemistry of the surface ocean is a nonlinear response to the atmospheric flux. The frequency of the depositions needs to be taken into account, because it will condition the impact of the deposited particles. This has large consequences on the time scales that have to be studied in order to get a realistic picture of the impact of dust deposition.

Supplementary material related to this article is available online at: http://www.biogeosciences-discuss.net/9/13857/2012/ bgd-9-13857-2012-supplement.zip.

Title Page

Abstract | Introduction

Conclusions | References

Tables | Figures

Back | Close

Full Screen / Esc

Printer-friendly Version

Interactive Discussion

References

Aguilar-Islas, A. M., Resing, J. A., and Bruland, K. W.: Catalytically enhanced spectrophotometric determination of manganese in seawater by flow-injection analysis with a commercially available resin for on-line preconcentration, Limnol. Oceanogr. Meth., 4, 105–113, doi:10.4319/lom.2006.4.105, 2006.

Baker, A. R. and Jickells, T. D.: Mineral particle size as a control on aerosol iron solubility, Geophys. Res. Lett., 33, L17608, doi:10.1029/2006gl026557, 2006.

Baker, A. R. and Croot, P. L.: Atmospheric and marine controls on aerosol iron solubility in seawater, Mar. Chem., 120, 4–13, doi:10.1016/j.marchem.2008.09.003, 2010.

Baker, A. R., Jickells, T. D., Witt, M., and Linge, K. L.: Trends in the solubility of iron, aluminium, manganese and phosphorus in aerosol collected over the Atlantic Ocean, Mar. Chem., 98, 43–58, doi:10.1016/j.marchem.2005.06.004, 2006.

Balistrieri, L., Brewer, P. G., and Murray, J. W.: Scavenging residence times of trace-metals and surface-chemistry of sinking particles in the deep ocean, Deep-Sea Res., 28, 101–121, 10.1016/0198-0149(81)90085-6, 1981.

Title Page

Abstract | Introduction

Conclusions | References

Tables | Figures

|◄ | ►|

◄ | ►

Back | Close

Full Screen / Esc

Printer-friendly Version

Interactive Discussion

Bonnet, S. and Guieu, C.: Dissolution of atmospheric iron in seawater, Geophys. Res. Lett., 31, L03303, doi:10.1029/2003gl018423, 2004.

Bonnet, S. and Guieu, C.: Atmospheric forcing on the annual iron cycle in the Western Mediterranean Sea: a 1-year survey, J. Geophys. Res.-Oceans, 111, 13, doi:10.1029/2005jc003213, 2006.

Boyle, E. A., Chapnick, S. D., Bai, X. X., and Spivack, A.: Trace-metal enrichments in the Mediterranean-Sea, Earth Planet. Sci. Lett., 74, 405–419, doi:10.1016/s0012-821x(85)80011-x, 1985.

Bressac, M., Guieu, C., Doxaran, D., Bourrin, F., Obolensky, G., and Grisoni, J.-M.: A mesocosm experiment coupled with optical measurements to assess the fate and sinking of atmospheric particles in clear oligotrophic waters, Geo-Mar. Lett., 32, 153–164, doi:10.1007/s00367-011-0269-4, 2012a.

Bressac, M., Guieu, C., Doxaran, D., Bourrin, F., and Leblond, N.: Lithogenic particle sinking and interactions with organic matter: implications on particulate organic carbon fluxes, Biogeosciences, in preparation, 2012b.

Bruland, K. W., Franks, R. P., Knauer, G. A., and Martin, J. H.: Sampling and analytical methods for the determination of copper, cadmium, zinc, and nickel at the nanogram per liter level in sea-water, Anal. Chim. Acta, 105, 233–245, doi:10.1016/s0003-2670(01)83754-5, 1979.

Brust, J. and Waniek, J. J.: Atmospheric dust contribution to deep-sea particle fluxes in the Subtropical Northeast Atlantic, Deep-Sea Res. Pt. I, 57, 988–998, doi:10.1016/j.dsr.2010.04.011, 2010.

Brust, J., Schulz-Bull, D. E., Leipe, T., Chavagnac, V., and Waniek, J. J.: Descending particles: from the atmosphere to the deep ocean; a time series study in the subtropical ne atlantic, Geophys. Res. Lett., 38, L06603, doi:10.1029/2010gl045399, 2011.

Buck, C. S., Landing, W. M., Resing, J. A., and Lebon, G. T.: Aerosol iron and aluminum solubility in the Northwest Pacific Ocean: results from the 2002 ioc cruise, Geochem. Geophy. Geosy., 7, Q04M07, doi:10.1029/2005gc000977, 2006.

Carr, M.-E., Friedrichs, M. A. M., Schmeltz, M., Noguchi Aita, M., Antoine, D., Arrigo, K. R., Asanuma, I., Aumont, O., Barber, R., Behrenfeld, M., Bidigare, R., Buitenhuis, E. T., Campbell, J., Ciotti, A., Dierssen, H., Dowell, M., Dunne, J., Esaias, W., Gentili, B., Gregg, W., Groom, S., Hoepffner, N., Ishizaka, J., Kameda, T., Le Quéré, C., Lohrenz, S., Marra, J., Mélin, F., Moore, K., Morel, A., Reddy, T. E., Ryan, J., Scardi, M., Smyth, T., Turpie, K., Tilstone, G., Waters, K., and Yamanaka, Y.: A comparison of global esti-

mates of marine primary production from ocean color, Deep-Sea Res. Pt. II, 53, 741–770, doi:10.1016/j.dsr2.2006.01.028, 2006.

Caschetto, S. and Wollast, R.: Vertical distribution of dissolved aluminium in the Mediterranean Sea, Mar. Chem., 7, 141–155, doi:10.1016/0304-4203(79)90006-9, 1979.

Chou, L. and Wollast, R.: Biogeochemical behavior and mass balance of dissolved aluminum in the Western Mediterranean Sea, Deep-Sea Res. Pt. II, 44, 741–768, doi:10.1016/s0967-0645(96)00092-6, 1997.

Copin-Montegut, G., Courau, P., and Nicolas, E.: Distribution and transfer of trace elements in the Western Mediterranean, Mar. Chem., 18, 189–195, doi:10.1016/0304-4203(86)90007-1, 1986.

Croot, P. L. and Johansson, M.: Determination of iron speciation by cathodic stripping voltammetry in seawater using the competing ligand 2-(2-thiazolylazo)-p-cresol (TAC), Electroanalysis, 12, 565–576, 2000.

Croot, P. L., Streu, P., and Baker, A. R.: Short residence time for iron in surface seawater impacted by atmospheric dry deposition from saharan dust events, Geophys. Res. Lett., 31, L23S08, doi:10.1029/2004gl020153, 2004.

Dammshäuser, A., Wagener, T., and Croot, P. L.: Surface water dissolved aluminum and titanium: tracers for specific time scales of dust deposition to the atlantic?, Geophys. Res. Lett., 38, L24601, doi:10.1029/2011gl049847, 2011.

Danielsson, L.-G., Magnusson, B., and Westerlund, S.: An improved metal extraction procedure for the determination of trace metals in sea water by atomic absorption spectrometry with electrothermal atomization, Anal. Chim. Acta, 98, 47–57, doi:10.1016/s0003-2670(01)83237-2, 1978.

Duce, R. A., Liss, P. S., Merrill, J. T., Atlas, E. L., Buat-Menard, P., Hicks, B. B., Miller, J. M., Prospero, J. M., Arimoto, R., Church, T. M., Ellis, W., Galloway, J. N., Hansen, L., Jickells, T. D., Knap, A. H., Reinhardt, K. H., Schneider, B., Soudine, A., Tokos, J. J., Tsunogai, S., Wollast, R., and Zhou, M.: The atmospheric input of trace species to the world ocean, Global Biogeochem. Cy., 5, 193, doi:10.1029/91gb01778, 1991.

Elbaz-Poulichet, F., Braungardt, C., Achterberg, E., Morley, N., Cossa, D., Beckers, J.-M., Nomérange, P., Cruzado, A., and Leblanc, M.: Metal biogeochemistry in the Tinto-Odiel Rivers (Southern Spain) and in the Gulf of Cadiz: a synthesis of the results of Toros project, Cont. Shelf Res., 21, 1961–1973, doi:10.1016/s0278-4343(01)00037-1, 2001.

Title Page

Abstract | Introduction

Conclusions | References

Tables | Figures

◀◀ | ▶▶

◀ | ▶

Back | Close

Full Screen / Esc

Printer-friendly Version

Interactive Discussion

Emerson, S., Quay, P., Karl, D., Winn, C., Tupas, L., and Landry, M.: Experimental determination of the organic carbon flux from open-ocean surface waters, Nature, 389, 951–954, 1997.

Fischer, A. C., Kroon, J. J., Verburg, T. G., Teunissen, T., and Wolterbeek, H. T.: On the relevance of iron adsorption to container materials in small-volume experiments on iron marine chemistry: 55Fe-aided assessment of capacity, affinity and kinetics, Mar. Chem., 107, 533–546, 2007.

Gledhill, M. and Buck, K. N.: The organic complexation of iron in the marine environment: a review, Front. Microbiol., 3, 69–86, doi:10.3389/fmicb.2012.00069, 2012.

Grasshoff, K., Kremling, K., and Ehrhardt, M. (Eds.): Methods of Seawater Analysis, Verlag Chemie, Weinheim, Germany, 1983.

Guerzoni, S., Molinaroli, E., Rossini, P., Rampazzo, G., Quarantotto, G., de Falco, G., and Cristini, S.: Role of desert aerosol in metal fluxes in the mediterranean area, Chemosphere, 39, 229–246, doi:10.1016/s0045-6535(99)00105-8, 1999.

Guieu, C., Duce, R., and Arimoto, R.: Dissolved input of manganese to the ocean: aerosol source, J. Geophys. Res., 99, 18789–18800, 1994.

Guieu, C., Loye-Pilot, M. D., and Ridame, C.: Dune – a dust experiment in a low nutrient, low chlorophyll ecosystem – quantifying the role of atmospheric input on marine ecosystem using large clean mesocosms, SOLAS Newslett., 9, 36–37, 2009.

Guieu, C., Dulac, F., Desboeufs, K., Wagener, T., Pulido-Villena, E., Grisoni, J.-M., Louis, F., Ridame, C., Blain, S., Brunet, C., Bon Nguyen, E., Tran, S., Labiadh, M., and Dominici, J.-M.: Large clean mesocosms and simulated dust deposition: a new methodology to investigate responses of marine oligotrophic ecosystems to atmospheric inputs, Biogeosciences, 7, 2765–2784, doi:10.5194/bg-7-2765-2010, 2010a.

Guieu, C., Loye-Pilot, M. D., Benyahya, L., and Dufour, A.: Spatial variability of atmospheric fluxes of metals (Al, Fe, Cd, Zn and Pb) and phosphorus over the whole Mediterranean from a one-year monitoring experiment: biogeochemical implications, Mar. Chem., 120, 164–178, doi:10.1016/j.marchem.2009.02.004, 2010b.

Guieu, C., Dulac, F., Ridame, C., and Pondaven, P.: An introduction to the dune project, Biogeosciences, in preparation, 2012.

Heller, M. I. and Croot, P. L.: Kinetics of superoxide reactions with dissolved organic matter in Tropical Atlantic surface waters near Cape Verde (Tenatso), J. Geophys. Res., 115, C12038, doi:10.1029/2009JC006021, 2010.

Title Page

Abstract | Introduction

Conclusions | References

Tables | Figures

|◄ | ►|

◄ | ►

Back | Close

Full Screen / Esc

Printer-friendly Version

Interactive Discussion

Honeyman, B. D., and Santschi, P. H.: Coupling adsorption and particle aggregation: laboratory studies of "colloidal pumping" using 59Fe-labeled hematite, Environ. Sci. Technol., 25, 1739–1747, 1991.

Honeyman, B. D., Balistieri, L. S., and Murray, J. W.: Oceanic trace metal scavenging: the importance of particle concentration, Deep-Sea Res., 35, 227–246, 1988.

Hunter, K. A.: The adsorptive properties of sinking particles in the deep ocean, Deep-Sea Res., 30, 669–675, 1983.

Hydes, D. J. and Liss, P. S.: Fluorimetric method for the determination of low concentrations of dissolved aluminium in natural waters, Analyst, 101, 922–931, 1976.

Hydes, D. J., de Lange, G. J., and de Baar, H. J. W.: Dissolved aluminium in the mediterranean, Geochim. Cosmochim. Acta, 52, 2107–2114, doi:10.1016/0016-7037(88)90190-1, 1988.

Jickells, T. D.: The inputs of dust derived elements to the sargasso sea; a synthesis, Mar. Chem., 68, 5–14, 1999.

Jickells, T., Church, T., Veron, A., and Arimoto, R.: Atmospheric inputs of manganese and aluminum to the sargasso sea and their relation to surface-water concentrations, Mar. Chem., 46, 283–292, doi:10.1016/0304-4203(94)90083-3, 1994.

Jickells, T. D., An, Z. S., Andersen, K. K., Baker, A. R., Bergametti, G., Brooks, N., Cao, J. J., Boyd, P. W., Duce, R. A., Hunter, K. A., Kawahata, H., Kubilay, N., laRoche, J., Liss, P. S., Mahowald, N., Prospero, J. M., Ridgwell, A. J., Tegen, I., and Torres, R.: Global iron connections between desert dust, ocean biogeochemistry, and climate, Science, 308, 67–71, doi:10.1126/science.1105959, 2005.

Johnson, K. S., Elrod, V., Fitzwater, S., Plant, J., Boyle, E., Bergquist, B., Bruland, K., Aguilar-Islas, A., Buck, K., Lohan, M., Smith, G. J., Sohst, B., Coale, K., Gordon, M., Tanner, S., Measures, C., Moffett, J., Barbeau, K., King, A., Bowie, A., Chase, Z., Cullen, J., Laan, P., Landing, W., Mendez, J., Milne, A., Obata, H., Doi, T., Ossiander, L., Sarthou, G., Sedwick, P., Van den Berg, S., Laglera-Baquer, L., Wu, J.-F., and Cai, Y.: Developing standards for dissolved iron in seawater, Eos Trans. AGU, 88, 131–132, 2007.

Journet, E., Desboeufs, K. V., Caquineau, S., and Colin, J.-L.: Mineralogy as a critical factor of dust iron solubility, Geophys. Res. Lett., 35, L07805, doi:10.1029/2007gl031589, 2008.

Klinkhammer, G. P.: Determination of manganese in sea water by flameless atomic absorption spectrometry after preconcentration with 8-hydroxyquinoline in chloroform, Anal. Chem., 52, 117–120, doi:10.1021/ac50051a028, 1980.

Title Page

Abstract | Introduction

Conclusions | References

Tables | Figures

|◀ | ▶|

◀ | ▶

Back | Close

Full Screen / Esc

Printer-friendly Version

Interactive Discussion

Kremling, K. and Petersen, H.: The distribution of zinc, cadmium, copper, manganese and iron in waters of the open Mediterranean Sea, Meteor. Forschungsergeb. Reihe A/B, 23, 5–14, 1981.

Laghdass, M., Blain, S., Besseling, M., Catala, P., Guieu, C., and Obernosterer, I.: Effects of saharan dust on the microbial community during a large in situ mesocosm experiment in the NW Mediterranean Sea, Aquat. Microb. Ecol., 62, 201–213, doi:10.3354/Ame01466, 2011.

Landing, W. M. and Paytan, A.: Marine chemistry special issue: aerosol chemistry and impacts on the ocean, Mar. Chem., 120, 1–3, doi:10.1016/j.marchem.2010.04.001, 2010.

Liu, X. and Millero, F. J.: The solubility of iron in seawater, Mar. Chem., 77, 43–54, 2002.

Longhurst, A., Sathyendranath, S., Platt, T., and Caverhill, C.: An estimate of global primary production in the ocean from satellite radiometer data, J. Plankton Res., 17, 1245–1271, doi:10.1093/plankt/17.6.1245, 1995.

Measures, C. I., Sato, T., Vink, S., Howell, S., and Li, Y. H.: The fractional solubility of aluminium from mineral aerosols collected in hawaii and implications for atmospheric deposition of biogeochemically important trace elements, Mar. Chem., 120, 144–153, doi:10.1016/j.marchem.2009.01.014, 2010.

Mendez, J., Guieu, C., and Adkins, J.: Atmospheric input of manganese and iron to the ocean: seawater dissolution experiments with saharan and north american dusts, Mar. Chem., 120, 34–43, doi:10.1016/j.marchem.2008.08.006, 2010.

Millot, C.: Circulation in the Western Mediterranean Sea, J. Marine Sys., 20, 423–442, doi:10.1016/s0924-7963(98)00078-5, 1999.

Mills, M. M., Ridame, C., Davey, M., La Roche, J., and Geider, R. J.: Iron and phosphorus co-limit nitrogen fixation in the Eastern Tropical North Atlantic, Nature, 429, 292–294, doi:10.1038/nature02550, 2004.

Milne, A., Landing, W., Bizimis, M., and Morton, P.: Determination of Mn, Fe, Co, Ni, Cu, Zn, Cd and Pb in seawater using high resolution magnetic sector inductively coupled mass spectrometry (HR-ICP-MS), Anal. Chim. Acta, 665, 200–207, doi:10.1016/j.aca.2010.03.027, 2010.

Moran, S. B. and Moore, R. M.: Temporal variations in dissolved and particulate aluminum during a spring bloom, Estuar. Coast. Shelf Sci., 27, 205–215, doi:10.1016/0272-7714(88)90090-x, 1988.

Morley, N. H., Burton, J. D., Tankere, S. P. C., and Martin, J. M.: Distribution and behaviour of some dissolved trace metals in the Western Mediterranean Sea, Deep-Sea Res. Pt. II, 44, 675–691, doi:10.1016/s0967-0645(96)00098-7, 1997.

Noble, A. E., Saito, M. A., Maiti, K., and Benitez-Nelson, C. R.: Cobalt, manganese, and iron near the hawaiian islands: a potential concentrating mechanism for cobalt within a cyclonic eddy and implications for the hybrid-type trace metals, Deep-Sea Res. Pt. II, 55, 1473–1490, doi:10.1016/j.dsr2.2008.02.010, 2008.

Obata, H., Shitashima, K., Isshik, K., and Nakayama, E.: Iron, manganese and aluminum in upper waters of the Western South Pacific Ocean and its adjacent seas, J. Oceanogr., 64, 233–245, 2008.

Pulido-Villena, E., Rerolle, V., and Guieu, C.: Transient fertilizing effect of dust in p-deficient lnlc surface ocean, Geophys. Res. Lett., 37, doi:10.1029/2009gl041415, 2010.

Ridame, C., Guieu, C., and L'Helguen, S.: Strong stimulation of N_2 fixation to saharan dust events: results from dust fertilizations in large mesocosms, Biogeosciences, in preparation, 2012.

Roitz, J. S. and Bruland, K. W.: Determination of dissolved manganese(ii) in coastal and estuarine waters by differential pulse cathodic stripping voltammetry, Anal. Chim. Acta, 344, 175–180, doi:10.1016/s0003-2670(97)00041-x, 1997.

Saito, M. A. and Moffett, J. W.: Temporal and spatial variability of cobalt in the Atlantic Ocean, Geochim. Cosmochim. Acta, 66, 1943–1953, doi:10.1016/s0016-7037(02)00829-3, 2002.

Sampling and sample-handling protocols for geotraces cruises: http://www.geotraces.org/libraries/documents/Intercalibration/Cookbook.pdf, last access: 08 October 2012, 2010.

Sañudo-Wilhelmy, S. A., Rivera-Duarte, I., and Russell Flegal, A.: Distribution of colloidal trace metals in the San Francisco Bay estuary, Geochim. Cosmochim. Acta, 60, 4933–4944, doi:10.1016/s0016-7037(96)00284-0, 1996.

Sarthou, G. and Jeandel, C.: Seasonal variations of iron concentrations in the ligurian sea and iron budget in the Western Mediterranean Sea, Mar. Chem., 74, 115–129, 2001.

Sedwick, P. N., Sholkovitz, E. R., and Church, T. M.: Impact of anthropogenic combustion emissions on the fractional solubility of aerosol iron: evidence from the Sargasso Sea, Geochem. Geophy. Geosy., 8, Q10Q06, doi:10.1029/2007gc001586, 2007.

Shelley, R. U., Zachhuber, B., Sedwick, P. N., Worsfold, P. J., and Lohan, M. C.: Determination of total dissolved cobalt in UV-irradiated seawater using flow injection with chemiluminescence detection, Limnol. Oceanogr. Meth., 8, 352–362, doi:10.4319/lom.2010.8.352, 2010.

Title Page

Abstract | Introduction

Conclusions | References

Tables | Figures

◄ | ►

◄ | ►

Back | Close

Full Screen / Esc

Printer-friendly Version

Interactive Discussion

Sherrell, R. M. and Boyle, E. A.: Zinc, chromium, vanadium and iron in the Mediterranean Sea, Deep-Sea Res. Pt. I, 35, 1319–1334, doi:10.1016/0198-0149(88)90085-4, 1988.

Spokes, L. J. and Jickells, T. D.: Factors controlling the solubility of aerosol trace metals in the atmosphere and on mixing into seawater, Aq. Geochem., 1, 355–374, doi:10.1007/bf00702739, 1996.

Statham, P. J., Burton, J. D., and Hydes, D. J.: Cd and Mn in the Alboran Sea and adjacent North Atlantic: geochemical implications for the Mediterranean, Nature, 313, 565–567, 1985.

Sunda, W. G. and Huntsman, S. A.: Microbial oxidation of manganese in a North Carolina estuary, Anglais, 32, 552–564, 1987.

Sunda, W. G. and Huntsman, S. A.: Effect of sunlight on redox cycles of manganese in the Southwestern Sargasso Sea, Deep-Sea Res. Pt. I, 35, 1297–1317, 1988.

Turekian, K. K.: The fate of metals in the oceans, Geochim. Cosmochim. Acta, 41, 1139–1144, doi:10.1016/0016-7037(77)90109-0, 1977.

van den Berg, C. M. G.: Evidence for organic complexation of iron in seawater, Mar. Chem., 50, 139–157, 1995.

van den Berg, C. M. G., Boussemart, M., Yokoi, K., Prartono, T., and Campos, M. L. A. M.: Speciation of aluminium, chromium and titanium in the nw mediterranean, Mar. Chem., 45, 267–282, doi:10.1016/0304-4203(94)90074-4, 1994.

Wagener, T., Pulido-Villena, E., and Guieu, C.: Dust iron dissolution in seawater: results from a one-year time-series in the mediterranean sea, Geophys. Res. Lett., 35, L16601, doi:10.1029/2008GL034581, 2008.

Wagener, T., Guieu, C., and Leblond, N.: Effects of dust deposition on iron cycle in the surface Mediterranean Sea: results from a mesocosm seeding experiment, Biogeosciences, 7, 3769–3781, doi:10.5194/bg-7-3769-2010, 2010.

Wagener, T., Bressac, M., Wuttig, K., and Guieu, C.: Changes in dust iron solubility after an artificial dust deposition in large mesocosms, Biogeosciences, in preparation, 2012.

Ye, Y., Wagener, T., Völker, C., Guieu, C., and Wolf-Gladrow, D. A.: Dust deposition: iron source or sink? A case study, Biogeosciences, 8, 2107–2124, doi:10.5194/bg-8-2107-2011, 2011.

Yoon, Y. Y., Martin, J. M., and Cotte, M. H.: Dissolved trace metals in the Western Mediterranean Sea: total concentration and fraction isolated by c18 sep-pak technique, Mar. Chem., 66, 129–148, doi:10.1016/s0304-4203(99)00033-x, 1999.

Zhuang, G., Yi, Z., Duce, R. A., and Brown, P. R.: Chemistry of iron in marine aerosols, Global Biogeochem. Cy., 6, 161, doi:10.1029/92gb00756, 1992.

Impacts of dust deposition on dissolved trace metal concentrations

K. Wuttig et al.

Title Page

Abstract	Introduction
Conclusions	References
Tables	Figures

|◄ ►|

◄ ►

Back Close

Full Screen / Esc

Printer-friendly Version

Interactive Discussion

Table 1. Total trace metal concentrations measured with the ETAAS.

Operation	Mesocosm	Depth (m)	Date and hour	Time (h)	Cd $(\mathrm{nmol\,l^{-1}})$	Co $(\mathrm{nmol\,l^{-1}})$	Cu $(\mathrm{nmol\,l^{-1}})$	Ni $(\mathrm{nmol\,l^{-1}})$	Pb $(\mathrm{nmol\,l^{-1}})$	Zn $(\mathrm{nmol\,l^{-1}})$
R1	C1	5	26 Jun 2010 10:00	−1	0.052	0.102	2.05	3.83	0.111	1.9
R1	C2	5	26 Jun 2010 10:00	−1	0.049	0.102	1.64	3.22	0.116	1.87
R1	C3	5	26 Jun 2010 10:00	−1	0.065	0.102	2.28	3.66	0.111	3.46
R1	D1	5	26 Jun 2010 10:00	−1	0.052	0.085	1.95	3.87	0.121	2.23
R1	D2	5	26 Jun 2010 10:00	−1	0.048	0.102	1.64	3.41	0.082	1.77
R1	D3	5	26 Jun 2010 10:00	−1	0.045	0.102	1.46	2.83	0.082	1.62
R1	OUT	5	26 Jun 2010 10:00	−1	NA	NA	NA	NA	NA	NA
R8	C1	5	2 Jul 2010 10:00	143	0.051	0.119	1.45	3.77	0.125	1.12
R8	C2	5	2 Jul 2010 10:00	143	0.051	0.102	1.87	3.58	0.116	1.7
R8	C3	5	2 Jul 2010 10:00	143	0.048	0.085	1.24	2.9	0.116	1.62
R8	D1	5	2 Jul 2010 10:00	143	0.052	0.102	1.81	3.6	0.053	3.26
R8	D2	5	2 Jul 2010 10:00	143	0.05	0.170	1.84	3.99	0.082	1.36
R8	D3	5	2 Jul 2010 10:00	143	0.058	0.119	1.92	3.68	0.097	1.64
R8	OUT	5	2 Jul 2010 10:00	143	0.052	0.119	1.42	3.34	0.087	1.01
R16	C1	5	9 Jul 2010 10:00	311	0.048	0.136	1.75	3.49	0.092	3.06
R16	C2	5	9 Jul 2010 10:00	311	0.048	0.136	1.81	3.8	0.116	1.12
R16	C3	5	9 Jul 2010 10:00	311	0.055	0.136	1.67	3.66	0.058	1.3
R16	D1	5	9 Jul 2010 10:00	311	0.049	0.153	2.16	3.94	0.106	3.62
R16	D2	5	9 Jul 2010 10:00	311	0.048	0.187	1.73	5.09	0.068	2.13
R16	D3	5	9 Jul 2010 10:00	311	0.053	0.153	1.59	3.85	0.087	1.91
R16	OUT	5	9 Jul 2010 10:00	311	0.052	0.136	1.61	3.78	0.101	1.15

Table 2. Trace metal concentrations before the start of the experiment.

	Concentration (nmol l^{-1}) INside the mesocosms	Concentration (nmol l^{-1}) OUTside the mesocosms
Al (FIA)	43.8 ± 1.4	36.97[a]
Cd (ETAAS)	0.0520 ± 0.007	0.05[b]
Co (ETAAS)	0.099 ± 0.007	0.12[b]
Cu (ETAAS)	1.83 ± 0.30	1.42[b]
Fe (FIA)	3.78 ± 0.67	4.44
Mn (FIA)	3.36 ± 0.37	3.50
Ni (ETAAS)	3.47 ± 0.40	3.34[b]
Pb (ETAAS)	0.104 ± 0.017	0.09[b]
Zn (ETAAS)	2.14 ± 0.67	1.01[b]

[a] This value was measured 47 h after the start of the experiment.
[b] These values were measured 143 h after the start of the experiment.

Table 3. Estimation of the elemental relative dissolution of dust in seawater.

		Mn	Fe	Al
	Elemental dust addition (μmol m^{-2})[a]	63.7	4136	15 271
First seeding	Difference of inventories Average DUST-Mesos minus average CONTROL-Mesos (μmol m^{-2})[b]	25.6	NA	128
	Dissolution (%)[c]	40	NA	0.84
	Time when DUST-Mesos inventories reached their maxima (h)	71	NA	47
Second seeding	Difference of inventories Average DUST-Mesos minus average CONTROL-Mesos (μmol m^{-2})[b]	28.6	4.9	284
	Dissolution (%)[c]	45	0.12	1.86
	Time when DUST-Mesos inventories reached their maxima (h)	239	191	215

[a] Estimation based on the addition of 10 g m^{-2} of dust with an elemental composition of Mn = 0.035 %, Fe = 2.31% and Al 4.12 % (Guieu et al., 2010a).
[b] Estimated with mean values for CONTROL-Mesos and DUST-Mesos.
[c] Estimated as the ratio between the difference of inventories and the amount of element added with dust.

Table 4. dMn, dFe and dAl dissolution and loss rates in $\mu mol\,m^{-2}\,d^{-1}$. They were calculated as the increase/decline of each metal in each of the DUST-Mesos by applying a linear regression to the inventory as a function of time. For the dissolution rates the calculation was started at the point before each of the seedings until the point of time when the concentration reached its maximum. For the loss rates the calculation was started at the point after each of the seedings when the concentration was the highest.

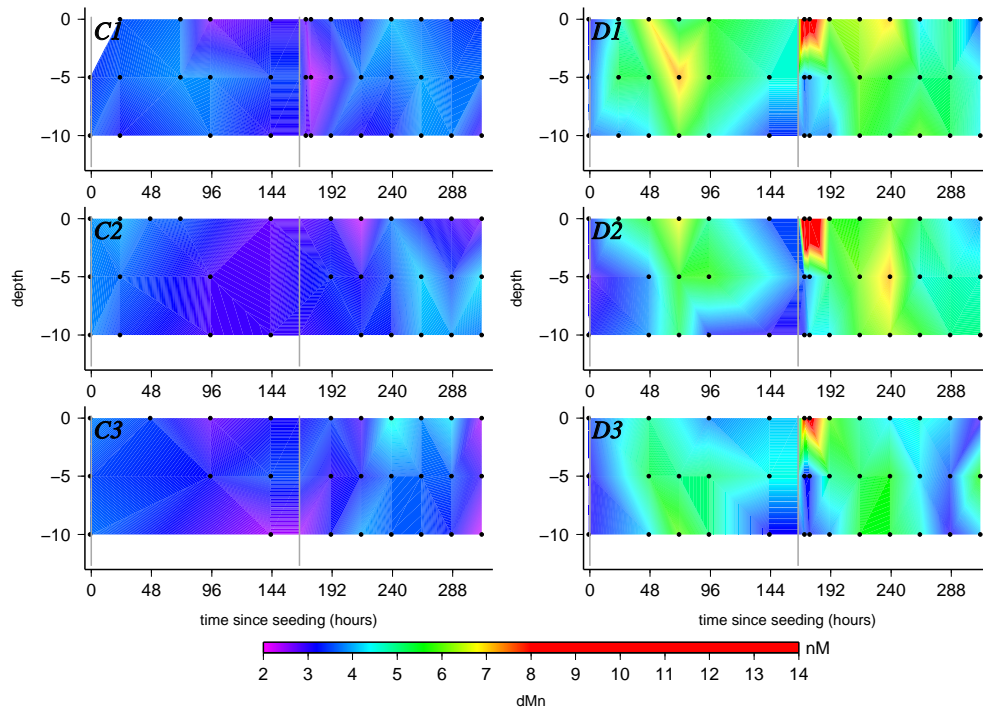| Dissolved trace metal	Seeding	Dissolution rates ($\mu mol\,m^{-2}\,h^{-1}$)	Operations used	Loss rate ($\mu mol\,m^{-2}\,d^{-1}$)	Operations used
dMn	1	0.43 ± 0.09	R1–R5	-0.35 ± 0.04	R5–8
dMn	2	0.27 ± 0.05	R8–R13	-0.25 ± 0.08	R13–16
	Control			-0.006 ± 0.013	R1–R16
dFe	1	NA	NA	NA	NA
dFe	2	0.67 ± 0.15	R9–11	NA	NA
	Control	NA	NA	-0.01 ± 0.01	R4–R16
dAl	1	2.8 ± 1.3	R1–R4	-0.07 ± 0.17	R4–R8
dAl	2	1.1	R8–R12	-1.9 ± 0.3	R12–R16
	Control			-0.24 ± 0.07	R1–R16

Fig. 1. Evolution of dissolved Manganese (dMn) in the 6 mesocosms (left CONTROL- and right hand side DUST-Mesos). The graphs are plotted as the time since the seeding (h) versus the depth (m) in the mesocosms. Black dots show the points were samples were taken. The two grey vertical bars highlight the time points when the fertilization took place (t0 and t166).
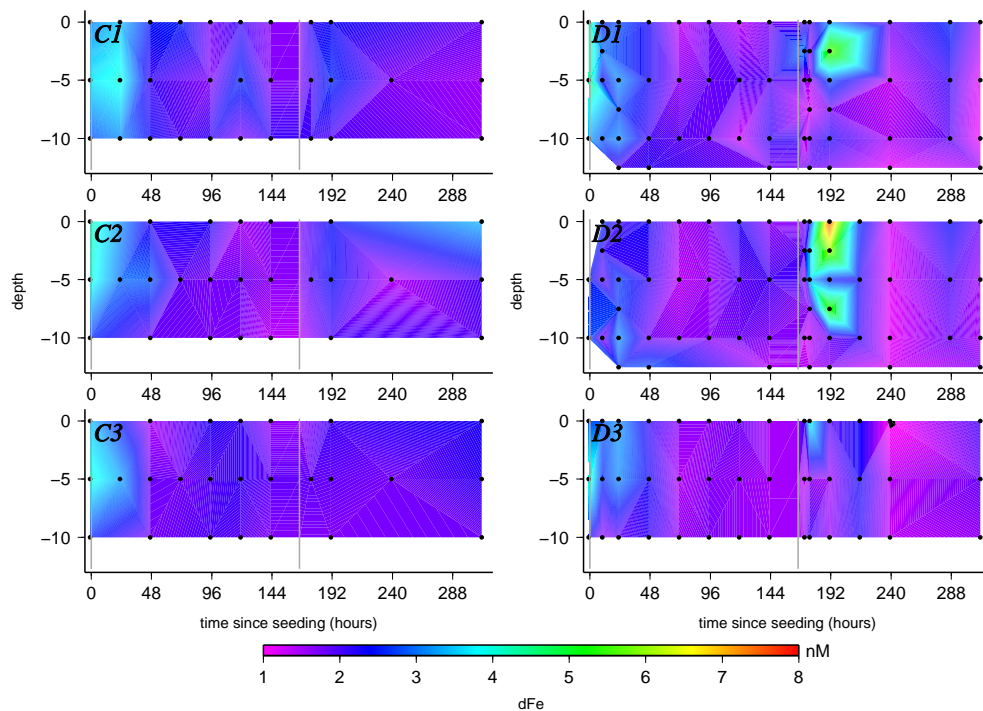
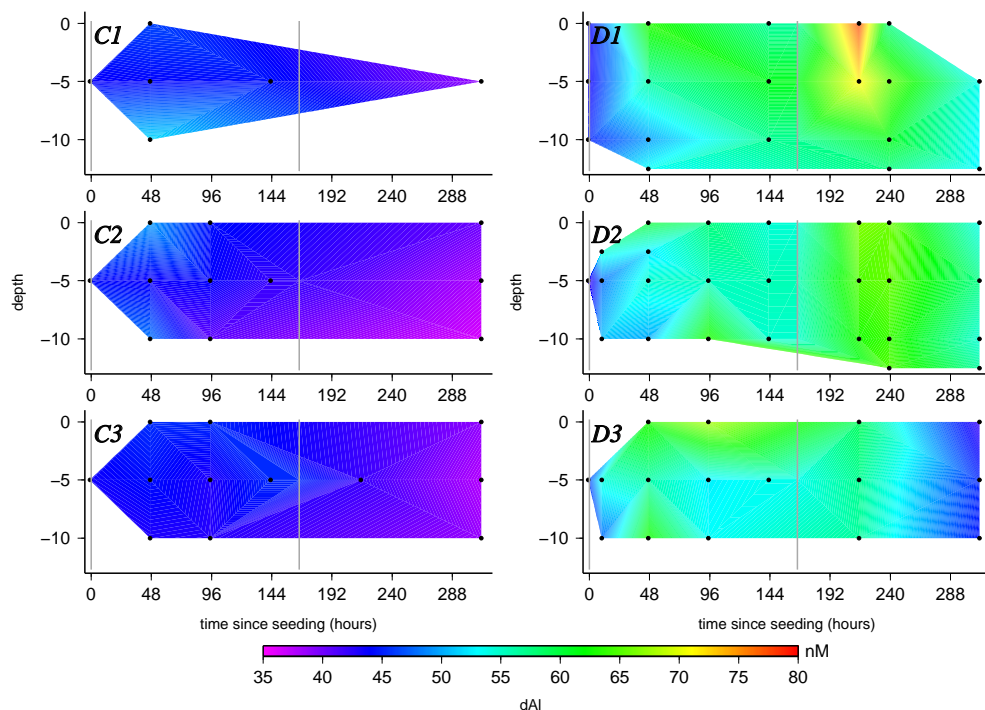**Fig. 2.** Evolution of dissolved Iron (dFe) in the 6 mesocosms. This graph is plotted in the same way as Fig. 1.

Fig. 3. Evolution of dissolved Aluminium (dAl) in the 6 mesocosms. This graph is plotted in the same way as Fig. 1.
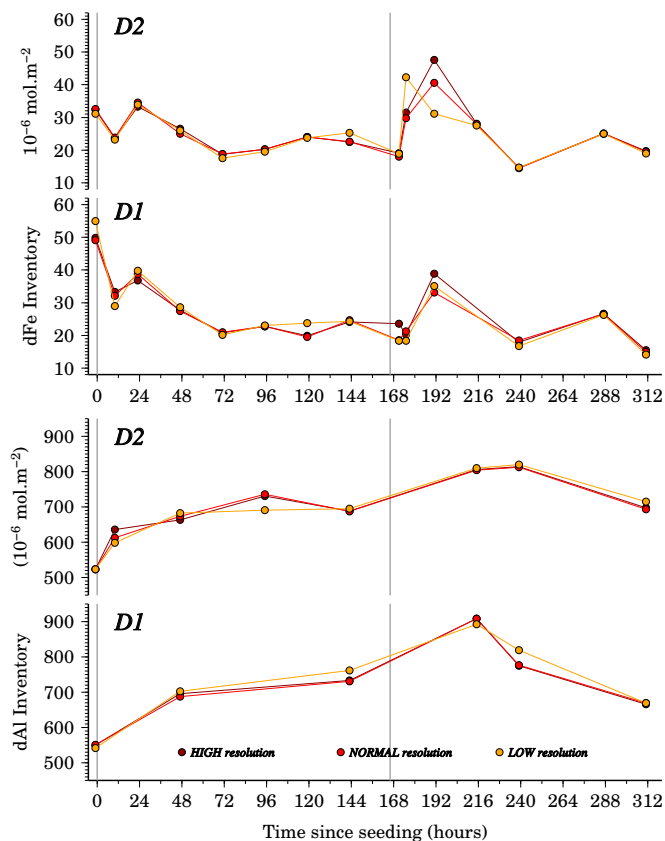
Fig. 4. Comparison of the 3 different resolutions (HIGH: dark red, 6 depths: 0.2, 2.5, 5, 7.5, 10, 12.5 m; NORMAL: light red, 3 depths: 0.2, 5 and 10 m; LOW: yellow, 1 depth: 5 m) for the two DUST-Mesos (D1 and D2) with 6 sampling depths for the inventories of dFe and dAl. The two grey vertical bars in each graph visualize the time points of the seeding.

Title Page

Abstract · Introduction

Conclusions · References

Tables · Figures

◀ · ▶

◀ · ▶

Back · Close

Full Screen / Esc

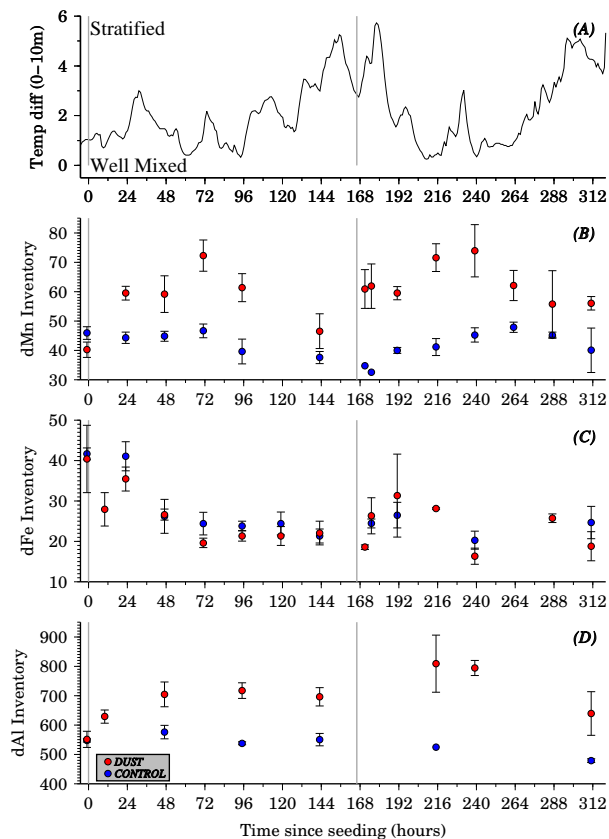Printer-friendly Version

Interactive Discussion

Fig. 5. Evolution of the temperature difference (0–10 m) **(A)** and the arithmetical means of the dissolved trace metal inventories (dMn **(B)**, dFe **(C)** and dAl **(D)** from top to bottom) of the DUST-Mesos (red circles) and the CONTROL-Mesos (blue circles).

Title Page

Abstract | Introduction

Conclusions | References

Tables | Figures

|◄ | ►|

◄ | ►

Back | Close

Full Screen / Esc

Printer-friendly Version

Interactive Discussion